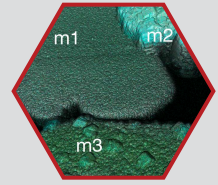


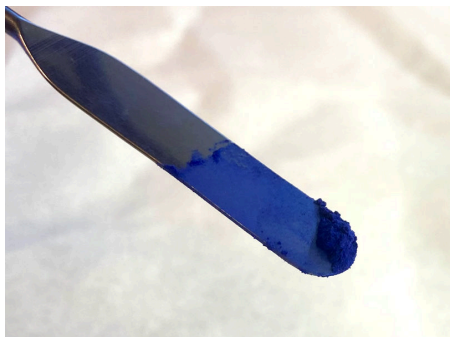
Pearlescent Pigment Analysis

Correlative SEM, AFM, and EDS measurements are used to compare mica- and borosilicate-based blue pearlescent pigments and to investigate how platelet morphology, nanoscale surface roughness, and elemental composition affect their resulting color and luster.

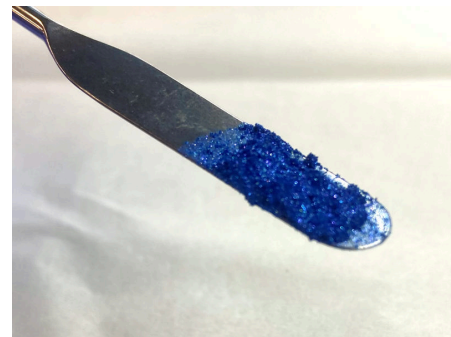


Pigments color our world and are used in a variety of consumer and industrial applications, including coatings, makeup, and paints. They are also used in consumables such as cereals, confections, chewing gum, and cocktails. Often, the striking appearance of these pigments is dictated by properties on micron-to-nanometer length scales. For example, the orientation of these pigments, how they are dispersed, and what coatings are applied, all have dramatic consequences on the perceived color and luster. These properties are also relevant for consumer safety [1], [2].

Through combining atomic force microscopy (AFM) with scanning electron microscopy (SEM), as performed in Quantum Design's FusionScope[®] system [3], measurements at various length scales can be seamlessly correlated. While the ultimate intent for a pigment is to have a strong effect optically, combining AFM with SEM can allow for a better understanding of the underlying mechanisms that govern the optical response. This Application Note presents a comparison of blue pearlescent pigments used in makeup manufacturing, one being a standard pearlescent pigment on mica compared to pigments on borosilicate glass from Glassflake[™], both shown in Figure 1. The mica pigment is marketed as having a softer matte finished, while the borosilicate pigment is designed for a shimmering sparkling finish, while both focus on a strong blue pigmentation.



(A)



(B)

Figure 1: Blue pearlescent pigment used in eyeshadow on small lab spatula, mica-based pigment (A) and borosilicate-based pigment (B).

Pearlescent Pigments

Pearlescent pigments are often made of naturally occurring mica that has then been coated with metal oxide nanoparticles to create a transparent but still sparkling flake [4]. This layered approach is a common manufacturing technique [5], [6]. These optical effects are critically dependent on the size of the mica platelets, with large platelets promoting specular reflections while smaller platelets exhibit a more diffusive response.

Additionally, the platelets' orientation and aggregation will also affect overall optical behavior. The more perpendicular these platelets are to the substrate the less reflective they appear, but they can still create a shimmering effect as the observer moves relative to the surface the pigments are on [7], [8], [9].

The concentration of these platelets also affects the orientation. If the platelet density is too high, they may agglomerate and prevent neighboring platelets from freely orienting. This can contribute to platelet orientations where edge scattering is more likely to occur, resulting in more diffuse reflections rather than the specular reflections associated with the sparkle of pearlescent pigments [10], [11], [12].

Finally, the coatings on the platelets themselves will have a strong effect; to achieve a sparkling effect, light must be able to pass through to the platelets to scatter. These coatings are typically made of metal oxides which have a higher index of refraction than the platelets causing the light to refract to different angles. Then when unpolarized white light passes through the optically anisotropic platelet, the different polarizations of light travel at different speeds resulting in a phase shift between them, this shift reduces some wavelengths of light and promotes others, this is called and interference color [13]. The thickness of the coating influences the color. These effects result in the sparkle seen in pearlescent pigments. Natural micas typically have a yellowish tint that can affect the final pigment color. To achieve highly saturated and pure colors additional absorption coatings are typically required. The thicker these absorption coatings are the less strong the specular reflections. By using borosilicate glass as a substrate, the pigments from Glassflake™ produce more specular reflections, as can be seen in Figure 1 (B) resulting in a brighter and more sparkly pigment. The smoothness of the substrate also means color travel effects are more prominent because the influence of viewing angle is not counteracted by terracing in the substrate.

Materials

Both pigments are interference effect pigments meaning they are an optically anisotropic platelet with a metal oxide coating where the thickness of the coating determines the coloring. In this case, both are coated with TiO₂ and SnO₂ to refract light at different angles. Additionally, they are both doped with ferric ferrocyanide, as a red light absorber, to further enhance blue coloration. See Table 1 for a comparison. Despite having very similar coatings, the different platelets affect the overall appearance. The mica platelets are made to be smaller, <20 μm to promote a softer more matte appearance. The borosilicate platelets are designed to be larger 20-100 μm to promote a more sparkling appearance.

	Mica	Borosilicate
Substrate	37-49%	69-80%
TiO ₂	51-59%	17-27%
SnO ₂	0-1%	0-1%
Ferric Ferrocyanide	0-1%	3-4%

Table 1: Composition percentages for the mica and borosilicate base pigments.

AFM with SEM

By utilizing the SEM (Figure 2) in the FusionScope, wide field images of the pigments can be obtained at high resolution, allowing quick identification of the platelets clustering. Additionally, these wide field views allow for the size of the platelets to be measured, providing an insight into their specular or diffuse reflection capabilities. The mica platelets (Figure 2 (A)) are on order 10-20 μm in length, while the borosilicate platelets (Figure 2 (B)) are typically larger at 30-60 μm . This makes sense as smaller pigments promote a more matte finish and larger pigments promote more specular reflections.

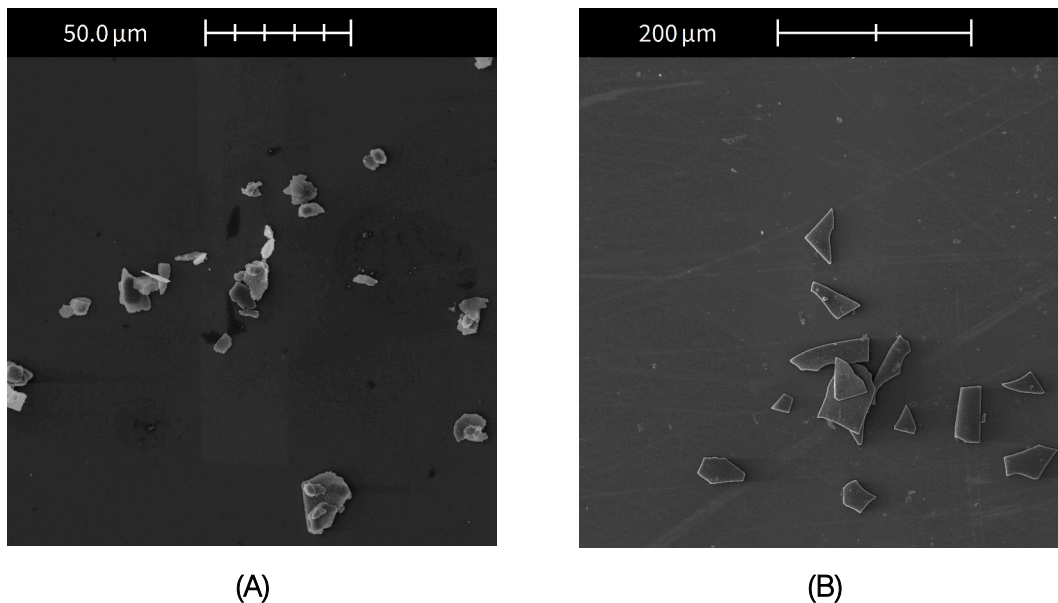


Figure 2: SEM of pearlescent pigments shows platelets grouping together with mica platelets (A) and borosilicate platelets (B).

The FusionScope features a tilting trunnion that allows it to rotate the sample and AFM head relative to the SEM column by up to 80 degrees to provide an angled view. This allows for a perspective view of the sample and AFM tip. By utilizing the tilting trunnion capabilities of the FusionScope, a better understanding of how these platelets are assembled on the substrate and how they stack on top of each other can be achieved. The platelets are often angled relative to the substrate, and the cubic structures on some of the mica platelets cause them to sit at an angle rather than lying flat (Figure 3 (A)). The tilted trunnion provides observation into how the smaller platelets stack on the larger ones. This is also critical for controllably positioning the AFM tip precisely on the smaller regions — something traditional optical microscopy would be unable to achieve at this length scale.

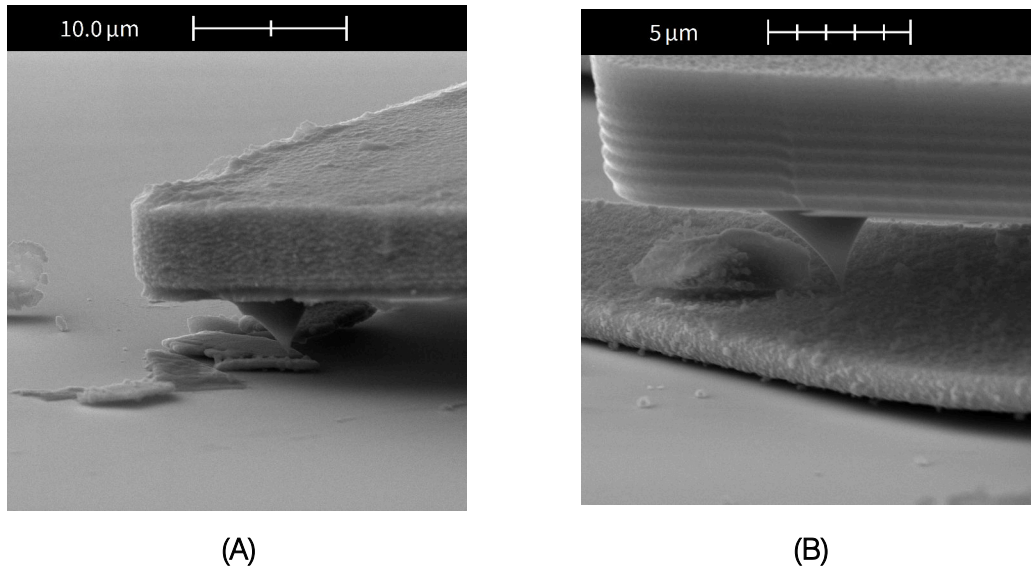


Figure 3: High-resolution SEM with trunnion tilted to 80 degrees to view the AFM tip positioned on mica (A) and borosilicate (B) platelet.

In **Figure 4 (A)**, three mica platelets are clustered together. Platelet m1 is covered in a regular bumpy texture likely due to small nanoparticles. Platelet m2 is dominated by small cubic structures, and platelet m3 shows the bumpy nanoparticle coating and few of the cubic structures. **Figure 4 (B)** shows several borosilicate platelets which all have consistent coatings, rather than the different levels of coatings seen on the mica platelets. In **Figure 4 (C)**, a closer view of the platelet in **Figure 4 (B)** can be seen, where the platelet appears to have a much more diffuse coating, notably lacking the cubic structures.

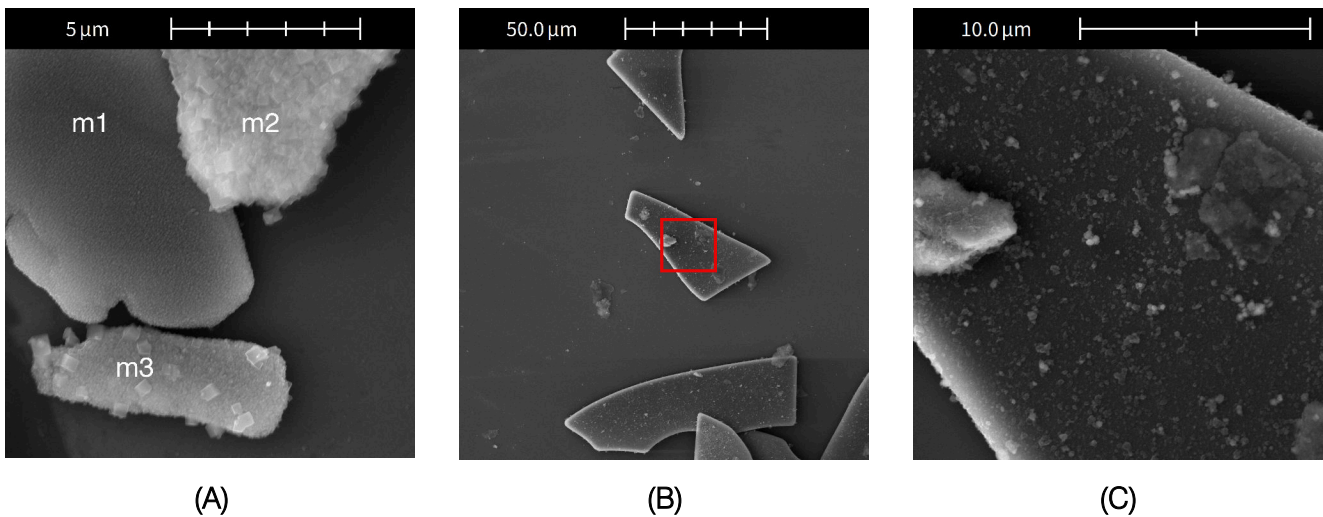


Figure 4: Top-down view of mica (A) and borosilicate (B and C) based pigments. (C) shows a zoomed in view of the red square in (B).

The FusionScope can then utilize AFM, to provide topographical information on the platelets to better relate the coating microstructure to the bulk optical properties. In **Figure 5 (A)** and **Figure 5 (B)**, the AFM can provide accurate sizing of the spherical TiO₂ nanoparticles (~100 nm diameter) and the cubic ferric

ferrocyanide (~400-600 nm) absorption pigment. **Figure 5 (B)** features a zoomed in view that shows layers of the densely packed TiO₂ nanoparticles. But the overall surface roughness looks to be related to concentration and aggregation of the cubic ferric ferrocyanide particles. Platelet m1 without the cubic structures is the smoothest with an Rq roughness ~50 nm while platelet m2 has the highest Rq roughness ~90 nm and platelet m3 with some cubic structures has an Rq roughness between those two, ~70 nm. The absorbing pigment concentration will contribute greatly to color intensity. But uneven aggregation produces a surface finish that suppresses coherent specular reflectance and hence produces a matte finish in bulk.

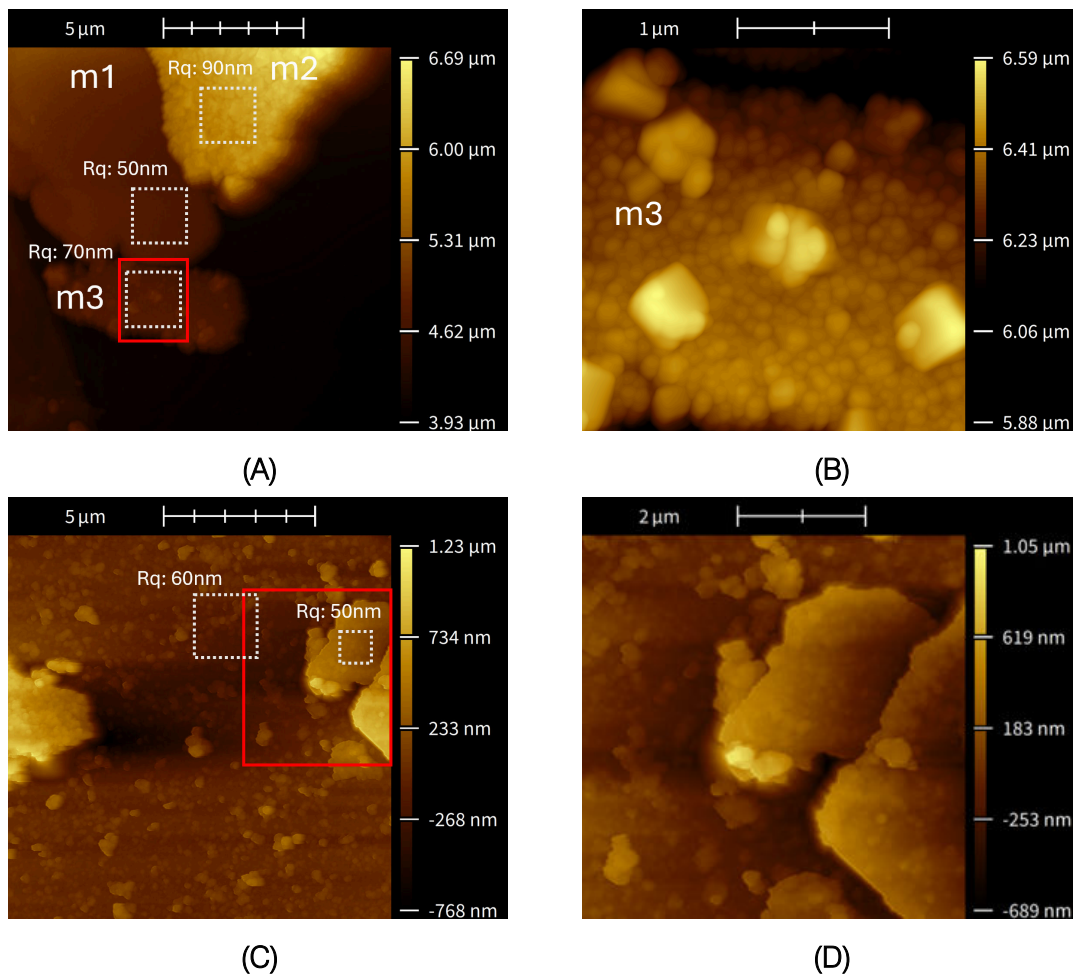


Figure 5: AFM images with quadratic mean roughness measurements in white dotted squares. **(A)** Topographical AFM scan of the mica pigment depicted in **Figure 4 (A)**. **(B)** A closer image of platelet m3, designated by the red box, showing both titanium dioxide nanoparticles (~100nm diameter) and ferric ferrocyanide crystals (400-600 nm edge). **(C)** Topographical AFM scan of borosilicate pigment depicted in **Figure 4 (C)**. **(D)** Shows a closer image of the feature on the right designated by the red box, showing the nanoparticle coating is sparser than in **(B)**.

These measurements can be compared to the AFM measurements performed on the borosilicate-based pigments in **Figure 5 (C)** and **Figure 5 (D)** where no cubic structures can be seen. The thicker absorption coating of ferric ferrocyanide on the mica platelets is likely needed to compensate for the yellowish tinge and natural terracing of the substrate. The distinction between spherical and cubic

nanoparticles is less apparent. The uniformity of the ferric ferrocyanide is better visualized by EDS (Figure 7). The variance in quadratic mean roughness (Rq) on the borosilicate platelets is much narrower at ~50-60 nm. The substrate smoothness and thickens uniformity allows for an equally uniform coating retaining sparkle and producing high color purity.

AFM with EDS

The FusionScope can utilize Energy Dispersive X-ray Spectroscopy (EDS), Figure 6, to better understand the elemental composition of the platelets and homogeneity of the pigment coatings.

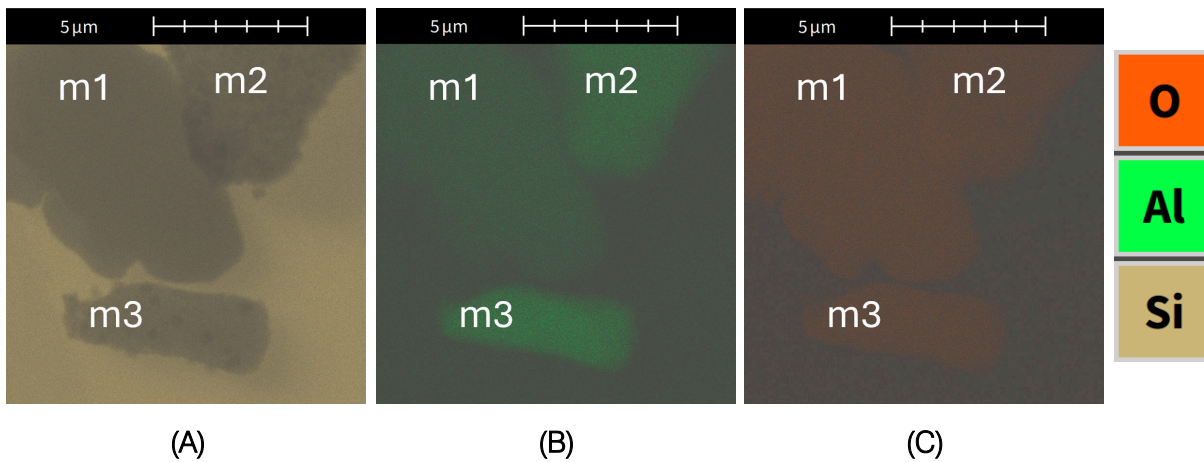


Figure 6: EDS shows that the mica platelets are primarily made of Si (A), Al (B), and O (C).

As shown in Figure 7 (A) and Figure 7 (C), both the mica and borosilicate platelets show Ti signal across their width, but with a slight increase in concentration towards the edges of the platelets illustrating it is indeed a coating. This tells us the small bumps are indeed titanium dioxide nanoparticles; a metal oxide commonly used in these pearlescent pigments.

Finally, in Figure 7 (B) and Figure 7 (D), the iron signal can be contrasted between the two platelet types. The small cubic features on the mica are the primary sources of Fe featuring a very strong localized Fe signature in the form of ferric ferrocyanide (Prussian Blue). Known for its cubic structure and incredibly strong blue pigmentation due to energy of the transfer of electrons from Fe(II) to Fe(III) [14]. In contrast, Fe signal on the borosilicate is more diffuse and while still featuring some areas of concentration around edges, is not as strictly localized to the cubic crystals seen on the mica. This is still ferric ferrocyanide but can be attributed to differences in both how the TiO₂ and ferric ferrocyanide nucleates during manufacturing. The exact manufacturing processes are proprietary. EDS can also be considered a highly matrix dependent analysis technique.

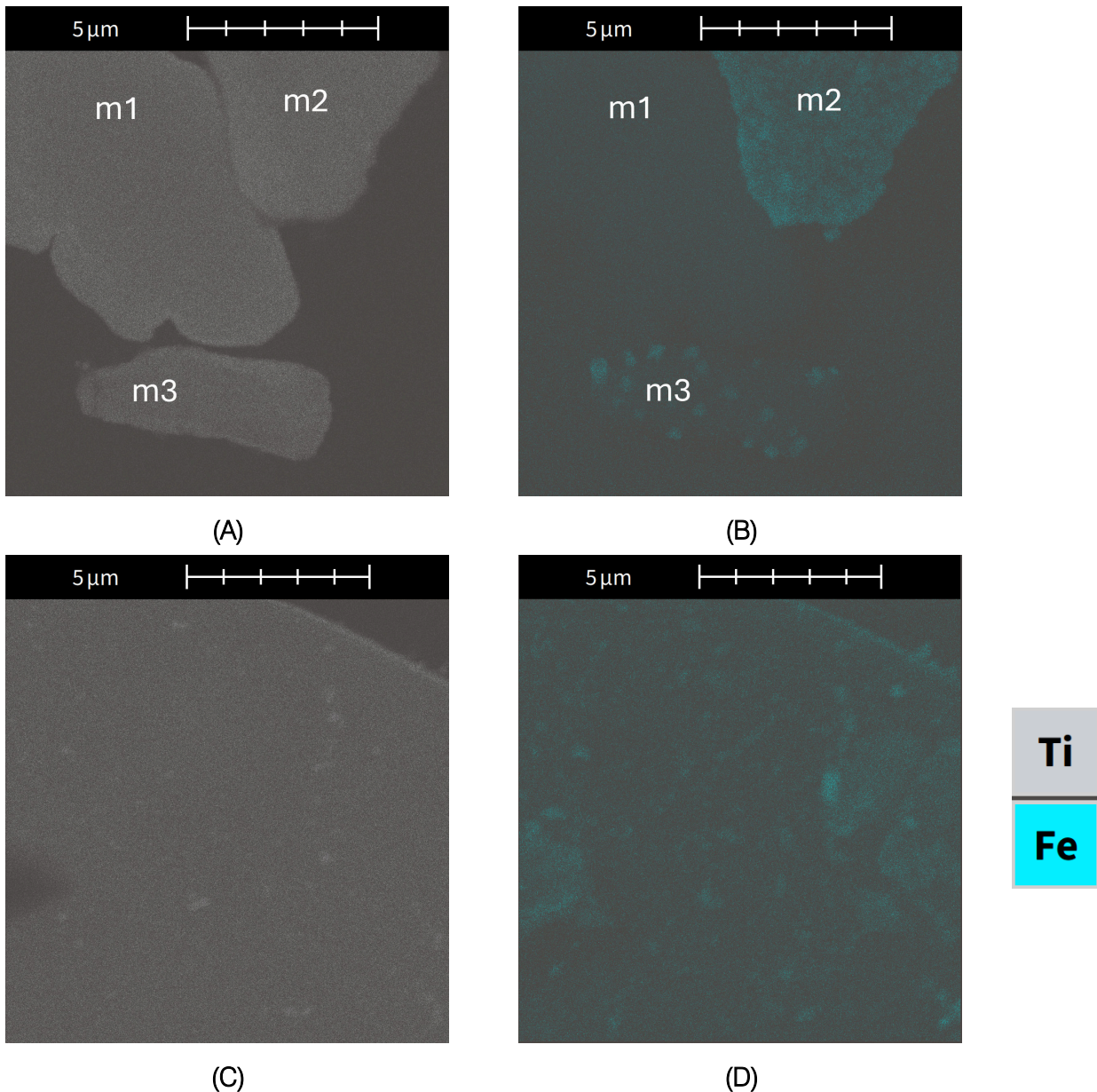


Figure 7: EDS of platelets showing distribution of additional coatings of titanium dioxide nanoparticles and ferric ferrocyanide. The mica platelets are (A) and (B) and borosilicate glass in (C) and (D).

The correlated AFM with EDS data, [Figure 8](#), is most useful in understanding how the microstructure of the coatings of titanium dioxide and ferric ferrocyanide relates to the bulk optical properties of the pigments. The correlated data shows that the Ti (coating) extends further than the Al (mica substrate) around the edges of the platelet, this is due to it being an external layer; by using the AFM data with the EDS overlaid on top we can get an idea for how this coating is built up around the edges of the platelet. The Ti signal extends roughly 300 nm past the Al substrate signal. This suggests the TiO_2 nanoparticle coating is on order 300 nm in thickness around the edges. This may be due to terracing around the edges of the mica platelets causing the TiO_2 nanoparticles to effectively fill up the terrace levels. The borosilicate glass platelets' Ti signal does not extend notably further than the flat platelet, this

alongside the AFM data showing a smoother surface, suggests a sparser coating. On the borosilicate glass the areas with higher Fe concentration tend to be in the form of much smaller clusters on the surface, or around edges, which is expected.

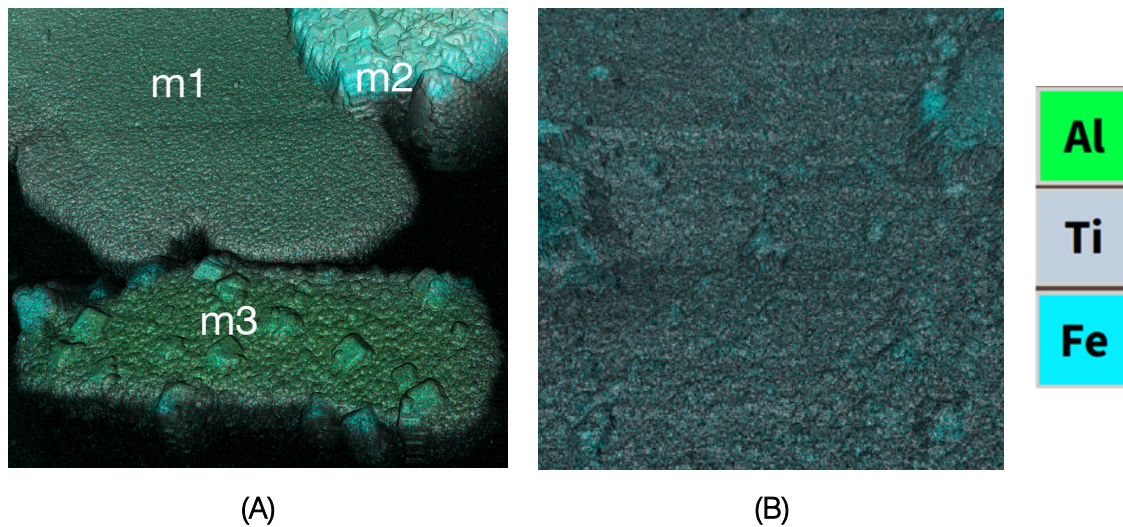


Figure 8: The correlated AFM-EDS data of mica **(A)** and borosilicate **(B)**. **(A)** The mica platelets show that the Ti extends further than the Al by about 300 nm, suggesting the thickness of the Ti nanoparticle layer is about 300 nm around the edges. **(B)** While the borosilicate pigment features some clustering of Fe, it is more thinly distributed than the ferric ferrocyanide crystals of the mica platelets.

Figure 8 (A) shows the three different platelets of the mica substrate-based pigment, each having dramatically different surface morphologies. The surface roughness can now be further correlated to the degree of ferric ferrocyanide coating. Platelet m2 is heavily coated in ferric ferrocyanide having large crystals of fairly uniform size but still contributing to a high surface roughness, $R_q = 90$ nm. This will contribute a deeply intense blue coloration but highly diffuse reflectance. Platelet m1 by contrast seemingly has very little ferric ferrocyanide producing a smooth surface, $R_q = 50$ nm. This would produce a whiter and brighter coloration as the TiO_2 coating interference mechanism will dominate in place of the strong absorption of the ferric ferrocyanide and the smoother surface produces more specular reflection. Platelet m3 is somewhat intermediate in the ferric ferrocyanide levels having randomly dispersed large crystals. The differing surface morphologies and compositions will contribute to the overall aggregated appearance of the pigment.

By contrast, the larger borosilicate platelets appear to have a much more homogeneous, finer coating of ferric ferrocyanide crystals producing a narrower surface roughness disparity, $R_q = 50-60$ nm. The result is that each flake produces a similar depth of color and individually have high specular reflection. Coupled with the substrate uniformity and transparency this maintains phase coherence. The aggregated appearance is highly lustrous and sparkly because of the individual relative orientations of the flakes.

Conclusion

The different measurement modes of the FusionScope have been demonstrated as comprehensive analytical toolset to study pigments. SEM allows users to quickly gather information on the size distribution, grouping, and orientation of the pigment platelets. By utilizing the SEM to quickly find the region of interest AFM can provide topographical information for the coatings used to create the interference effect. Furthermore, EDS allows for elemental mapping of these coatings to guide the AFM to inhomogeneous regions. This combination can further categorize the coating homogeneity and distinguish additional absorbance pigment dopants, in this case ferric ferrocyanide. The correlative microscopy and spectroscopy offered by FusionScope is not only convenient but also reduces sampling artifacts for more accurate assessments to explain bulk optical properties of the pigment.

References

- [1] G. O'Hanlon, "Understanding Pigment Particles: Effects on Gloss, Tinting Strength, and Durability," 2024. <https://www.naturalpigments.com/artist-materials/pigment-particle-size-role-in-art>.
- [2] Van Horn, Metz & Co., "What Are Pearlescent Pigments & How Do They Work," 2022. <https://www.vanhornmetz.com/what-are-pearlescent-pigments/>.
- [3] Quantum Design, Inc., "FusionScope® by Quantum Design — A New AFM-SEM Correlative Microscopy Platform," <https://fusionscope.com/>.
- [4] Q. Cheng, et al., "Synthesis of novel colored substrate-free pearlescent pigments of vanadium phosphates with large-size layered platelet morphology," *Journal of Alloys and Compounds*, **2025**, 1010, 177735, <https://doi.org/10.1016/j.jallcom.2024.177735>.
- [5] P. Cao, C. Lavallee, S. Jones and D. Cacace, "Synthetic mica based pearlescent pigments containing ferrites". Patent EP2052035A2, 2007.
- [6] A. Vorster, "Innovative technology delivers pure pearlescent pigments with unrivalled effects," *Pharmaceutical & Cosmetic Review*, **2021**, 48, no. 8, pp. 10-11, https://issuu.com/newmediab2b/docs/pcr_aug_21_/s/13028274.
- [7] See reference [2].
- [8] See reference [4].
- [9] E. Kirchner and J. Houweling, "Measuring flake orientation for metallic coatings," *Progress in Organic Coatings*, **2009**, 64, no. 2, pp. 287-293, [10.1016](https://doi.org/10.1016/j.porgcoat.2009.06.016).
- [10] See reference [2].
- [11] See reference [4].
- [12] See reference [9].
- [13] C. Oleari, "Color in optical coatings," in *Optical Thin Films and Coatings*, Second ed., A. Piegari and F. Flory, Eds., Woodhead Publishing, 2018, pp. 389-421, <https://doi.org/10.1016/B978-0-08-102073-9.00009-6>.
- [14] E. Reguera, E. Marín, A. Calderón and J. Rodríguez-Hernández, "Photo-induced charge transfer in Prussian blue analogues as detected by photoacoustic spectroscopy," *Spectrochimica Acta Part A: Molecular and Biomolecular Spectroscopy*, **2007**, 68, no. 1, pp. 191-197, <https://doi.org/10.1016/j.saa.2006.11.013>.